Environmental Science and Pollution Research (2022) 29:45885–45902
https://doi.org/10.1007/s11356-022-19130-0

RESEARCH ARTICLE

Design and application of molecularly imprinted polymers for adsorption and environmental assessment of anti-inflammatory drugs in wastewater samples

Jessica Meléndez-Marmolejo[1] · Lorena Díaz de León-Martínez[1] · Vanessa Galván-Romero[1] · Samantha Villarreal-Lucio[1] · Raúl Ocampo-Pérez[2] · Nahum A. Medellín-Castillo[3] · Erika Padilla-Ortega[2] · Israel Rodríguez-Torres[4] · Rogelio Flores-Ramírez[5]

Received: 10 November 2021 / Accepted: 4 February 2022 / Published online: 12 February 2022

Abstract

In this study, a series of molecularly imprinted polymers (MIPs) have been synthesized using separately diclofenac, naproxen, and ibuprofen as templates with three different polymerization approaches. Two functional monomers, methacrylic acid (MAA) and 2-vinylpyridine (2-VP), were tested and ethylene glycol dimethacrylate (EGDMA) was used as crosslinker; also, template-free polymers (NIPs) were synthesized. It was found that the MIP with the highest retention percentage for diclofenac was the one prepared by the emulsion approach and with MAA (98.3%); for naproxen, the one prepared by the bulk polymerization with MAA (99%); and for ibuprofen, the one synthesized by bulk with 2-VP (97.7%). These three MIPs were characterized by scanning electron microscopy, thermogravimetric test, Fourier transform infrared, specific area measurements, and surface charge. It was found that the emulsion method allowed particle size control, while the bulk method gave heterogeneous particles. The three evaluated MIPs exhibited thermal stability up to 300 °C, and it was observed that 2-VP confers greater stability to the material. From the BET analysis, it was demonstrated that the MIPs and NIPs evaluated are mesoporous materials with a pore size between 10 and 20 nm. In addition, the monomer influenced the surface charge of the material, since the MAA conferred an acidic point of zero charge (PZC), while the 2-VP conferred a PZC of basic character. Through adsorption isotherms, it was determined that there is a higher adsorption capacity of the MIPs at acidic pH following a pseudo-second-order kinetic model. Finally, the MIPs were used to determine the non-steroidal anti-inflammatory drugs (NSAIDs) understudy in San Luis Potosí, México, wastewater, finding concentrations of 0.642, 0.985, and 0.403 mg L^{-1} for DCF, NPX, and IBP, respectively.

Keywords Molecularly imprinted polymers · Diclofenac · Naproxen · Ibuprofen · Wastewater treatment

Responsible Editor: Tito Roberto Cadaval Jr

✉ Rogelio Flores-Ramírez
rfloresra@conacyt.mx

[1] Centro de Investigación Aplicada en Ambiente Y Salud (CIAAS), Avenida Sierra Leona No. 550, CP 78210, Colonia Lomas Segunda Sección, San Luis Potosí, SLP, México

[2] Centro de Investigación Y Estudios de Posgrado, Facultad de Ciencias Químicas, Universidad Autónoma de San Luis Potosí, San Luis Potosí 78260, México

[3] Centro de Investigación Y Estudios de Posgrado, Facultad de Ingeniería, Universidad Autónoma de San Luis Potosí, San Luis Potosí, SLP 78290, México

[4] Instituto de Metalurgia-Facultad de Ingeniería, UASLP, Av. Sierra Leona 550, Lomas 2ª Sección, 78210 San Luis Potosí, SLP, México

[5] CONACYT Research Fellow, Coordinación Para La Innovación Y Aplicación de La Ciencia Y La Tecnología (CIACyT), UASLP, Av. Sierra Leona 550, Lomas 2ª Sección, 78210 San Luis Potosí, SLP, México

Introduction

Pharmaceutical compounds represent an environmental concern because of their presence in aquatic ecosystems, leading to ecotoxicological effects (Parolini 2020). In addition, due to their extensive use for diseases treatments in humans and animals, wastewater discharges from municipal systems present high concentrations of these compounds and their metabolites, leading to harmful effects on the environment shortly (Eslami et al. 2015).

Among pharmaceuticals, non-steroidal anti-inflammatory drugs (NSAIDs) diclofenac (DCF), naproxen (NPX), and ibuprofen (IBP) are the most frequently detected and distributed drugs in the environment (Świacka et al. 2021; Wojcieszyńska and Guzik 2020). For example, for DCF, Bonnefille et al. reported a review of the presence of this compound in water and aquatic organisms, finding concentrations in water ranging from 50 ng L^{-1} to 3000 ng L^{-1} (Bonnefille et al. 2018). Several adverse effects have been reported from exposure to NSAIDs in aquatic species. For example, IBP was reported to cause an increase in the activity of some antioxidant and biotransformation enzymes in zebrafish (Bartoskova et al. 2013). In addition, an alteration in biochemical biomarkers and DNA damage in *Daphnia magna* species has also been reported by exposure to DCF, NPX, and IBP (Gómez-Oliván et al. 2014). It has been reported that the elimination of NSAIDs in wastewater treatment plants (WWTP) is inefficient; as a consequence, they are discharged directly into water resources, reaching levels that produce effects on aquatic organisms such as hormonal effects on their reproduction, oxidative stress, and genotoxicity (Gani et al. 2021; Islas-Flores et al. 2017; Madikizela and Ncube 2021; Parida et al. 2021).

There are significant challenges in removing and monitoring NSAIDs in complex environmental matrices such as wastewater. Regarding monitoring, the most commonly used analytical methodologies for identification and quantification are high-performance liquid chromatography (HPLC) and spectrophotometric methods (Kot-Wasik et al. 2007). In most cases, the determination of NSAIDs involves a pre-concentration step followed by separation and quantification usually performed by liquid chromatographic methods (Paíga et al. 2015).

Research in the environmental field increasingly relies on specific and sensitive analytical methods, which must detect and quantify trace and ultra-trace pollutants in very complex matrices; sample preparation is a key step for the assessment of pollutants; this step includes the pre-concentration of the analyte and the removal of the matrix effect which allows to obtain lower detection limits and increase sensibility and selectivity. Studies on the quantification of NSAIDs in different environmental matrices have focused on the development of methods such as solid phase extraction (Zhou et al. 2021), solid phase microextraction (Shamsayei et al. 2018), and ultrasound-assisted dispersive liquid–liquid microextraction (Qiao et al. 2016), among others.

Among these techniques, solid phase extraction is one of the most widely used sample pre-concentration techniques due to the diversity of adsorbents, high pre-concentration capacity and recovery. According to the literature, the use of molecularly imprinted polymers (MIPs) as a highly selective adsorbent material is a promising approach for the quantification of emerging contaminants in complex matrices (Madikizela et al. 2018).

These adsorbents are three-dimensional synthetic materials with pores or cavities to specifically retain a molecule of interest; MIPs are synthesized in the presence of this template (analyte of interest), which gives the polymer the specific shape, arrangement, orientation, and bonds to selectively retain it, which after being removed from the binding sites leaves the empty cavities to be re-occupied by the analyte or a highly related compound (chemical family of the analyte). Although MIPs have been used in areas that require high selectivity such as chromatographic methods, sensors, and contaminant removal, the use as highly selective extraction materials is the most widely used application (Azizi and Bottaro 2020), because it exhibits low cost, easy preparation, reversible adsorption and desorption, thermal, mechanical, and chemical stability (de Leon-Martinez et al. 2020).

Therefore, this work's main objective was to synthesize and characterize molecularly imprinted polymers to selectively remove IBP, NPX, and DCF in an aqueous solution. Furthermore, the adsorption process was studied at different solution pH to evaluate the adsorption mechanism, and an analysis and quantification method of the three compounds is also proposed. Finally, the materials developed were used to pre-concentrate and quantify the presence of NSAIDs in wastewater from the city of San Luis Potosí, México.

Materials and methods

All reagents, methacrylic acid (MAA), 2-vinylpyridine (2-VP), ethylene glycol dimethacrylate (EDGMA), azobisisobutyronitrile (AIBN), polyvinyl alcohol (PVA), lauryl sulfate (SDS), formic acid, diclofenac (DCF) sodium, and naproxen (NPX) were purchased from Sigma-Aldrich (Darmstadt, Germany). The organic solvents, methanol, and toluene were obtained from Tedia Company Inc. (Fairfield, Ohio, USA). Hydrochloric acid (HCl) and potassium hydroxide (KOH) were supplied by Merck (State of Mexico).

Synthesis of molecularly imprinted polymers

The synthesis of the polymers was carried out with slight modifications of those reported in previous works of our research group (Diaz de León-Martínez et al. 2018), under three non-covalent approaches.

(i) Emulsion polymerization First, PVA (1.55 g) and SDS (0.1078 g) were dissolved in hot water (75 mL) in a flat-bottomed flask with stirring by a magnetic stir bar at 250 rpm under an inert nitrogen atmosphere (99.9% purity) and hermetically sealed. Then, in another flask, the pre-polymerization mixture was prepared, template molecule (DCF 60 mg, NPX 50 mg, or IBP 40 mg) and functional monomer (MAA 85 µL or 2-VP 110 µL) dissolved in methanol (2 mL) and porogen (toluene, 4 mL). Crosslinker (EDGMA, 2 mL) and initiator (AIBN, 150 µL) were added to this mixture and stirred with a magnetic stir bar at 250 rpm until complete dissolution. Subsequently, the pre-polymerization mixture was added droplet by droplet by syringe to the above mixture; the reaction was kept at a constant temperature of 70 °C in a glycerin bath with continuous stirring at 100 rpm for 24 h. Finally, the polymer was obtained and washed with hot water to remove PVA and SDS residues.

(ii) Bulk polymerization First, the templates (DCF 60 mg, NPX 50 mg, or IBP 40 mg) were mixed with the monomer (MAA 85 µL or 2-VP 110 µL) in a reaction flask with magnetic stirring at 250 rpm until homogeneous, and then, methanol (2 mL), crosslinker (EDGMA, 2 mL), initiator (AIBN, 150 µL), and porogen (toluene, 4 mL) were added; the crosslinker (EDGMA, 2 mL), the initiator (AIBN, 150 µL), and the porogen (toluene, 4 mL) were added; the reaction was carried out under an inert nitrogen atmosphere without agitation at 70 °C in a glycerin bath for 24 h.

(iii) Co-precipitation polymerization This method consists of the same procedure and reaction conditions as the bulk polymerization, but with the addition of 5 times the porogen (toluene, 20 mL) and solvent (methanol 10 mL), with constant magnetic stirring at 100 rpm at 70 °C for 24 h.

The non-imprinted polymers (NIPs) were prepared in the same way as the corresponding MIPs but without the presence of the template molecule.

The obtained polymers were crushed in a mortar and sieved to a particle size of 250 µm. For cleaning of the template molecule in the MIPs, ten washing cycles were used with 10 mL of methanol in 0.1% 0.1 N HCl; each cycle was sonicated for 10 min and centrifuged at 2500 rpm for 5 min; the polymers were recovered and weighed to establish the reaction yield.

Determination of NSAIDs by HPLC–DAD

The determination of DCF, NPX, and IBP was performed by diode-array high-performance liquid chromatography (HPLC-DAD) (Agilent 1260 Infinity Series) at a wavelength of 220 nm. The separation was carried out through an Eclipse XDB C_{18} column (4.6 × 250 mm, 5 µm). The mobile phase consisted of 40% ortho-phosphoric acid (pH 2.6) and 60% acetonitrile in an isocratic flow rate at 1 mL min^{-1} for 10 min with a sample injection volume of 20 µL.

The validation of the analytical method was carried out based on the guide for the validation of analytical methods for the determination of organic compounds at trace level (AOAC/FAO/IAEA/IUPAC 2000) by assessing the following parameters: limit of detection (LOD) and quantification (LOQ), linearity (R^2), sensibility, and precision. Linearity was expressed by the correlation coefficient (R^2) and sensitivity determined by the slope of the working range curve (LOQ—2 mg L^{-1}) obtained from the average of seven curves; precision was obtained by repeatability (evaluating three curves in one day) and reproducibility (obtained from 7 calibration curves over three days). The limit of detection (LOD) was determined using the blank analysis method using the following formula: $LOD = X + 3SD_{blank}$. The limit of quantification was calculated in concentration units as $LOQ = LOD = X + 10SD_{blank}$.

Determination of the retention percentages

NPX, DCF, and IBP retention assays on the synthesized MIPs were performed by packing 20 mg of each MIP into 6 mL solid-phase extraction cartridges, and then, 1 mL of loading solution was added at a concentration of 2 mg L^{-1} of the corresponding NSAIDs used as the template for each imprinted polymer. The eluent of each loading was analyzed by HPLC–DAD, and the retention percentage (%*R*) was calculated with the following equation:

$$\%R = \frac{C_o - C_f}{C_o} \times 100\%, \quad (1)$$

where C_o is the initial concentration of each NSAID in the load (mg L^{-1}) and C_f is the eluent concentration in each load (mg L^{-1}). Subsequently, the MIP with the highest retention percentage for each NSAID was selected for further analysis.

Morphological characterization of MIPs/NIPs

Micrographs of the MIPs and NIPs were obtained using a field emission scanning electron microscope (FE-SEM)

FEI model Inspect F50 to evaluate the surface and morphology of all the polymers obtained.

Thermogravimetric analysis

The thermogravimetric analysis was performed using a thermogravimetric analyzer (TGA), PerkinElmer, model Pyris Diamond TGA/DTA in the presence of nitrogen (60 mL min^{-1}). The temperature profile programmed to the TGA consisted of two processes that occurred in series, first a drying process of the sample at 105 °C and then the pyrolysis process that took place by increasing the sample temperature up to 600 °C at 10 °C min^{-1}.

Infrared spectroscopy

The functional groups of the materials were evaluated by FT-IR Fourier transform infrared spectroscopy (Thermo Scientific, Nicolet iS10 model). Infrared spectra were collected in a spectral range from 500 to 4000 cm^{-1}.

Textural properties

The textural properties of the materials were obtained from nitrogen adsorption–desorption measurements at 77 K using an automatic adsorption instrument (Autosorb-IQ, Quantachrome Instrument Corp., Boynton Beach, FL, USA). The specific surface area (S_{BET}) was calculated using the BET method. Barrett, Joyner, and Halenda's (BJH) method was used to calculate the pore size distributions.

Surface charge distribution and point of zero charge

The surface charge of MIPs and NIPs was determined by the acid–base titration proposed by Kuzin and Loskutov (1996). For this purpose, 50 mL of neutralizing solutions with pH between 2 and 12 was prepared by adding various volumes between 0.2 and 10 mL of titrated solutions of HCl and NaOH, both at a concentration of 0.1 N. The solutions were then volumetrically titrated with a 0.1 N NaCl solution.

In a centrifuge tube, 0.1 g of MIP or NIP and 25 mL of the different neutralizing solutions were added; likewise, 25 mL of each solution was placed in centrifuge tubes that were left as blanks. Every 30 min, each tube was agitated until 2 h, and at the end, the pH was evaluated, and then, the potentiometric curves of the blank, MIP, and NIP were plotted.

The surface charge was calculated with the equation

$$C_s = \frac{C_N\left(V_B - V_A\right)}{m} \times F, \tag{2}$$

where C_s is the surface charge of the adsorbent at a given pH value (C g^{-1}), C_N is the concentration of the neutralizing solution (mol L^{-1}), V_A is the volume of 0.1 N NaOH or HCl solution used to reach a given pH value in the experiment using the adsorbent (L), V_B is the volume of 0.1 N NaOH or HCl solution to reach a given pH value in the experiment using the adsorbent (L), V_B is the volume of 0.1 N NaOH or HCl solution used to reach a given pH value in the experiment without adsorbent (L), m is the mass of MIP or NIP (g), and F is the Faraday constant (96,485 C mol^{-1}).

Adsorption kinetics and isotherms

The Freundlich and Langmuir isotherm models have been widely used in fitting adsorption equilibrium data of organic compounds in the aqueous phase. Redlich-Peterson R is a three-parameter isotherm model that results from a combination of the Freundlich and Langmuir model (Soto et al. 2011). These models were used to fit the adsorption equilibrium data and their equations are shown below.

$$q = kC^{1/n}, \tag{3}$$

$$q = \frac{q_m KC}{1 + KC}, \tag{4}$$

$$q = \frac{aC}{1 + bC^{\beta}}, \tag{5}$$

where C (mg L^{-1}) is the adsorbate concentration at equilibrium, q_m (mg L^{-1}) is the maximum adsorption capacity, K (L mg^{-1}) is the affinity constant related to the adsorption energy, k ($mg^{1-1/n}$ $L^{1/n}$ g^{-1}) is a constant related to the adsorption capacity of the adsorbent, the constant n indicates the adsorption intensity, and a (L g^{-1}), b (L $mg^{-1})^{\beta}$, and b are constants of the Redlich-Peterson isotherm.

Concentrations in the range of 1 to 500 mg L^{-1} were used for the isotherms, and all experiments were performed at 24 °C. The equilibrium adsorption capacity, q (mg g^{-1}), was calculated according to the equation

$$q = \frac{V\left(C_o - C\right)}{W}, \tag{6}$$

where C_o (mg L^{-1}) is the initial adsorbate concentration and V (L) and W (g) are the volume of the standard solutions and the weight of the polymer, respectively.

The kinetic study was performed following the retention assay methodology and determining the concentration of each free NSAID in the supernatant at time intervals with an initial concentration of 10 mg L^{-1}.

The kinetic test data were analyzed using the pseudo-first and pseudo-second-order equations. The pseudo-first-order (PFO) and pseudo-second-order (PSO) equations are shown below, respectively:

$$q_t = q_e\left(1 - e^{-k_1 t}\right), \tag{7}$$

$$q_t = \frac{k_2 q_e^2 t}{1 + k_2 q_e t}, \tag{8}$$

where q_e and q_t (mg g^{-1}) are the amounts of adsorbate bound to the adsorbent at equilibrium and at time t (min), respectively, and k_1 (min^{-1}) and k_2 (g mg^{-1} min^{-1}) are the PFO and PSO model constants, respectively.

To fit the experimental data to the analyzed mathematical models, Statistica® version 7.0 software was used, and the best-fitting model was chosen because of the correlation coefficient (R^2) closest to 1.

Imprinting factor

To verify the selectivity of each of the MIPs against the template for which they were designed, a mixture containing DCF, NPX, and IBP, all at a concentration of 2 mg L^{-1} in Milli-Q water pH 6, was prepared. 1 mL of this mixture was then passed through each of the MIPs following the retention assay methodology. Similarly, the NIPs were analyzed to compare them to their corresponding MIP.

The specificity of MIPs and NIPs was estimated by the partition coefficient of the NSAIDs between polymer and solution. The partition coefficient was calculated by the following equation:

$$K_D = \frac{q_e}{C} = \frac{q_e}{C_o(1 - (\%R/100))}, \tag{9}$$

where C_p (mg L^{-1}) is the amount of analyte bound to the MIP or NIP and C_s (mg L^{-1}) is the concentration of each analyte remaining in the loading eluent. Also, the imprinting factor (IF) was used to evaluate the selectivity of each MIP against the template for which it was synthesized in the presence of the other NIPs similar in structure. The IF was calculated with the following equation:

$$\mathrm{IF} = \frac{K_{\mathrm{MIP}}}{K_{\mathrm{NIP}}}, \tag{10}$$

where K_{MIP} and K_{NIP} represent the partition coefficients of the compounds understudy for the MIP and NIP, respectively. Additionally, the addition of sulfamethoxazole and metronidazole at 1 mg L^{-1} was performed to verify interferences with organic molecules not similar to NSAIDs.

MIPs for the determination of NSAIDs in wastewater

For the pilot study, five raw wastewater samples were obtained at the following locations: Camino a San Juanico el Chico, Periférico Norte, San Luis Potosí, coordinates 22°13′24.6″N 100°59′19.1″W. These water samples came from the locations' communities, and 1 L of raw water was collected at 1 m depth. Temperature (25 °C) and pH were recorded at the sampling site (7.1), and then, pH was adjusted to 2 with HCl to prevent the growth of microorganisms. Finally, the sample was frozen until analysis.

Columns of 50 mL were packed with 50 mg of each MIP to pre-concentrate DCF, NPX, and IBP. 40 mL of wastewater was passed through each column, and then, 4 mL of MeOH was added as elution. Finally, this eluent was filtered with 0.45 µm PTFE filters, and each elution was analyzed by HPLC–DAD. In parallel, the same methodology was followed, but sampling 40 mL of synthetic water containing 1 mL of a mixture of 1 mg L^{-1} of each NSAID at pH 6. Each experiment was performed in triplicate at 24 °C.

Results and discussion

Synthesis of imprinted and non-imprinted polymers

A total of 18 MIPs and 6 NIPs were obtained (6 MIPs per template molecule) (Table 1). Between 1.5 and 2 g of polymer were obtained for the co-precipitation and bulk methods, and between 0.8 and 1 g were obtained for the emulsion method. The cleanup of the MIPs was analyzed by HPLC to verify the absence of each one of the NSAIDs. Figure 1 presents a chromatogram of the fifth wash of the MIP for DCF synthesized by emulsion using MAA as monomer and the chromatogram in the tenth wash, where it is observed the absence of the DCF peak that corroborates that the MIP was free of the template; this was proven for each NSAID, found that at wash 7 and 8 it was free of NXP and IPB, respectively. This result is interesting as it indicates the appropriate conditions for recovery for MIP as a function of the concentration of the NSAIDs; thus, lower concentrations require less solvent volume for MIP regeneration. This has been reported in MIPs of MAA with a β-cyclodextrin template where they observed that in 3 washes of 30 mL of MeOH and water, regeneration of the polymer is achieved (Wang et al. 2019).

The validation of the method was obtained from the calibration curves for each NSAID obtained from 0.05 to 2 mg L^{-1}. In addition, linearity for all NSAIDs was verified with the R^2 value being greater than 0.999; a limit of detection of 0.029 mg L^{-1}, 0.018 mg L^{-1}, and 0.057 mg L^{-1} for DCF, NPX, and IBP, respectively; and a limit of quantification of 0.18, 0.11, and 0.33 mg L^{-1} for DCF, NPX, and IBP, respectively.

Figure 2 shows an example chromatogram showing the retention times for NPX at 4.8 min, DCF at 7.9 min, and IBP at 9.1 min.

Table 1 Code of the MIPs and NIPs synthesized for DCF, NPX, and IBP

Code	Template (AINE)	Polymerization method	Monomer	Polymer
ME-DCF-01	DCF	Emulsion	Methacrylic acid	MIP
ME-DCF-02	DCF	Emulsion	Vinylpyridine	MIP
MB-DCF-03	DCF	Bulk	Methacrylic acid	MIP
MB-DCF-04	DCF	Bulk	Vinylpyridine	MIP
MC-DCF-05	DCF	Co-precipitation	Methacrylic acid	MIP
MC-DCF-06	DCF	Co-precipitation	Vinylpyridine	MIP
ME-NPX-01	NPX	Emulsion	Methacrylic acid	MIP
ME-NPX-02	NPX	Emulsion	Vinylpyridine	MIP
MB-NPX-03	NPX	Bulk	Methacrylic acid	MIP
MB-NPX-04	NPX	Bulk	Vinylpyridine	MIP
MC-NPX-05	NPX	Co-precipitation	Methacrylic acid	MIP
MC-NPX-06	NPX	Co-precipitation	Vinylpyridine	MIP
ME-IBP-01	IBP	Emulsion	Methacrylic acid	MIP
ME-IBP-02	IBP	Emulsion	Vinylpyridine	MIP
MB-IBP-03	IBP	Bulk	Methacrylic acid	MIP
MB-IBP-04	IBP	Bulk	Vinylpyridine	MIP
MC-IBP-05	IBP	Co-precipitation	Methacrylic acid	MIP
MC-IBP-06	IBP	Co-precipitation	Vinylpyridine	MIP
NIP-E1	–	Emulsion	Methacrylic acid	NIP
NIP-E2	–	Emulsion	Vinylpyridine	NIP
NIP-B3	–	Bulk	Methacrylic acid	NIP
NIP-B4	–	Bulk	Vinylpyridine	NIP
NIP-C5	–	Co-precipitation	Methacrylic acid	NIP
NIP-C6	–	Co-precipitation	Vinylpyridine	NIP

MIP molecularly imprinting polymer, *NIP* non-molecularly imprinting polymer

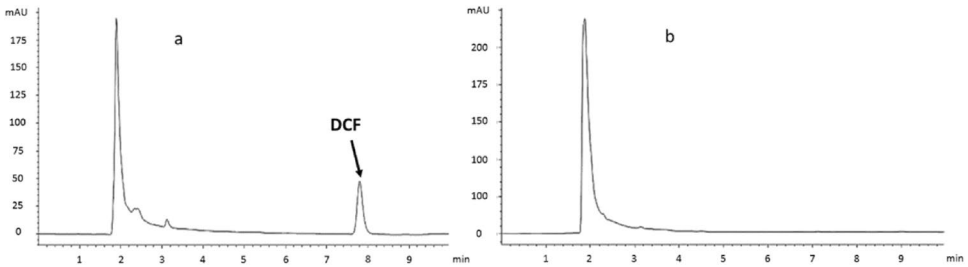

Fig. 1 Chromatograms of MIP washes. **a** Fifth wash of ME-DCF-01. **b** Tenth wash of ME-DCF-01

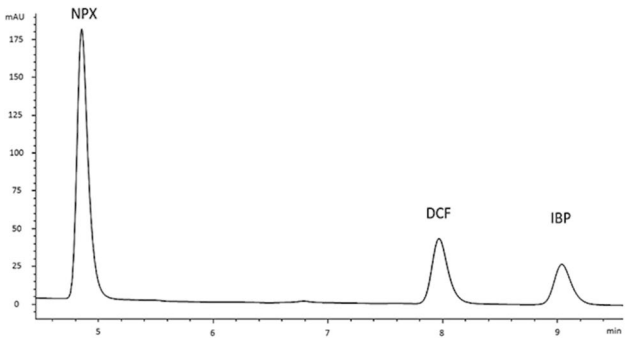

Fig. 2 Chromatogram of a mixture of DCF, NPX, and IBP at 2 mg L^{-1}

Retention percentages

Figure 3a shows the retention percentages obtained for the MIPs of DCF, NPX, and IBP. The MIP synthesized by the emulsion method for DCF (ME-DCF-01) and bulk for NPX (MB-NPX-03), both prepared with methacrylic acid (MAA) as a monomer, obtained the highest retention percentages of 98.3% and 99.0%, respectively. Concerning their NIPs (NIP-E1, NIP-B3), they reached between 50 and 58%.

The MIP with the IBP template with the highest percentage retention was synthesized in bulk using 2-VP as the monomer (MB-IBP-04), with an IBP retention of

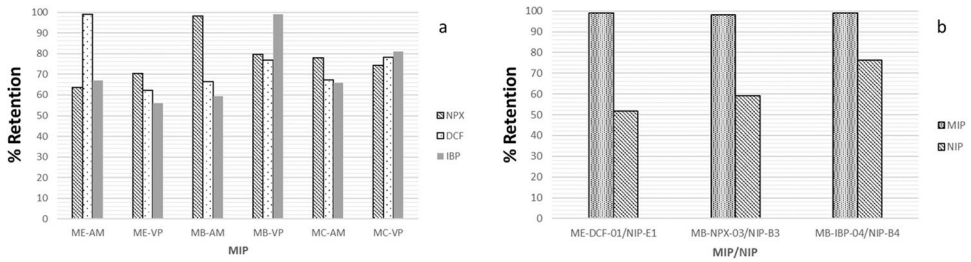

Fig. 3 **a** Retention rates of the synthesized MIPs for DCF, NPX, and IBP. **b** Comparison of the retention rate between the MIPs with the highest retention and their corresponding NIPs

97.7%. The corresponding NIP (NIP-B4) showed a lower IBP retention of 78.9%, proving the increased adsorption by molecular imprinting on the polymeric matrix.

Figure 3b shows the comparison of the retention percentages of the MIPs with their corresponding NIPs (NIP-E1, NIP-B3, and NIP-B4); it can be observed a difference in the results obtaining retention values of the NIPs, due to the imprinting of the template molecules. In other studies, it has already been observed that NIPs have adsorption capacity; however, the recovery of the analyte is generally lower than that of the imprinted polymer, which proves the effect of molecular imprinting (Liu et al. 2020; Zheng et al. 2018). Thus, high retention percentages were considered as selection factors of the MIPs for the following tests.

Morphological characterization by scanning electron microscopy

Micrographs obtained for DCF MIP and NIP, both synthesized by emulsion, are shown in Fig. 4a, b. The images show spherical particles for both MIP and NIP, with a size up to 1 µm. This particle shape is commonly obtained in emulsion-synthesized polymers; this technique allows to control how the polymer is created within the micelles in solution (Chen et al. 2015).

In Fig. 4c, d, micrographs are presented for the polymers MB-NPX-03 and MB-IBP-04, both mass-synthesized, for which agglomerated particles (cauliflower-shaped) of irregular and heterogeneous size were observed. These characteristics were also present in their corresponding NIPs.

Since both MIPs and NIPs have similar morphology when synthesized by the same method, this may indicate that the presence of DCF, NPX, or IBP in the polymer matrix does not interfere with the obtained morphology of the polymers. The morphologies are due to monomer-crosslinker-porogen interaction; Renkecz et al. (2014) showed that in copolymerization using MAA-EGDMA and toluene as solvent, the growth of cauliflower-shaped microparticles probably proceeds with the enthalpic precipitation mechanism that is usually observed in low solvency media (Renkecz et al. 2014).

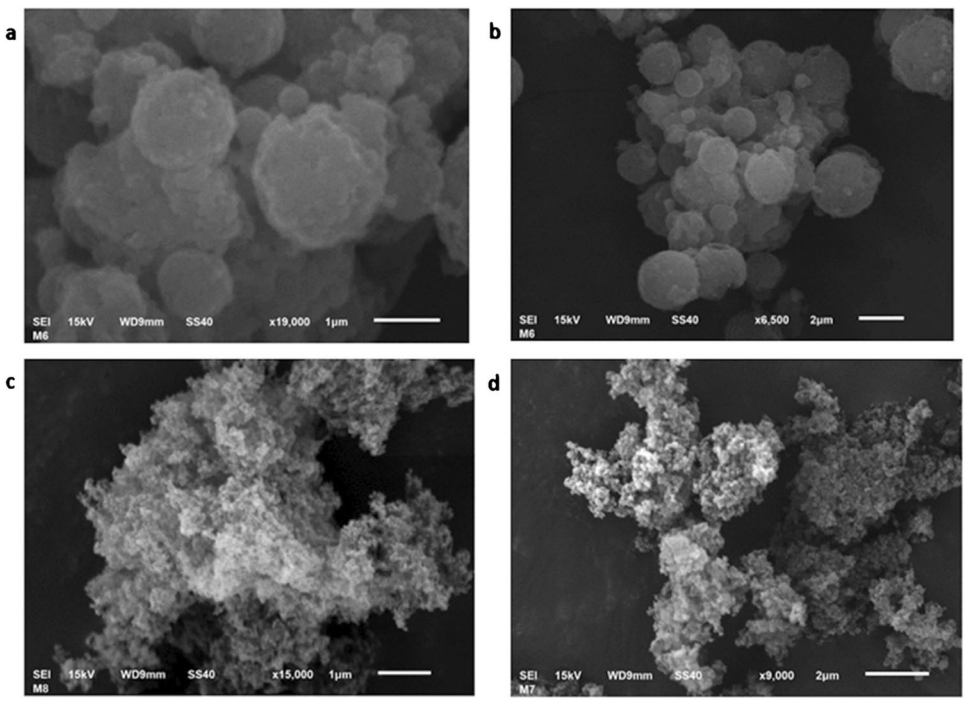

Fig. 4 Scanning electron microscope images. **a** ME-DCF-01. **b** NIP-E1. **c** MB-NPX-03. **d** MB-IBP-04

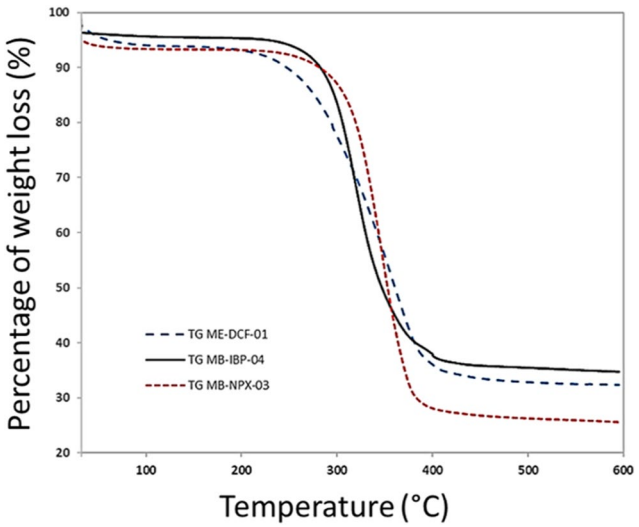

Fig. 5 TGA curves for the imprinted polymers: ME-DCF-01, MB-NPX-03, and MB-IBP-04

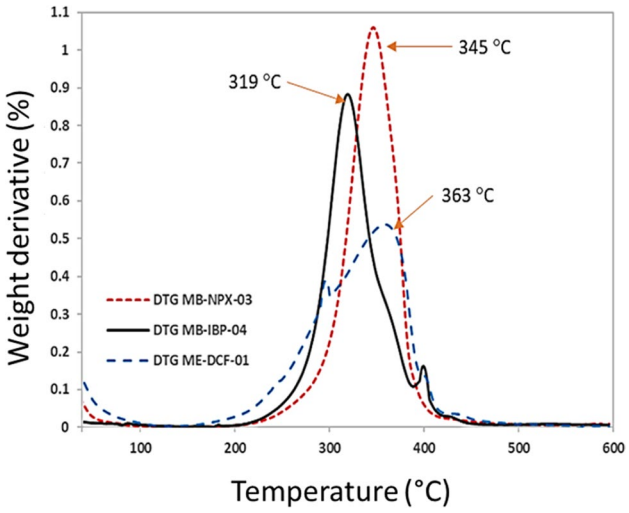

Fig. 6 dML analysis for the imprinted polymers: ME-DCF-01, MB-NPX-03, and MB-IBP-04

Thermogravimetric analysis

Figure 5 shows the mass loss (ML) curves for each evaluation. All the polymers lose water in the initial step, up to approximately 100 °C. The MB-NPX-04 polymer was the least stable, presenting the highest weight loss up to 75% at 400 °C. It was observed that MB-IBP-04 was the most stable MIP with a weight loss of 60% at 400 °C; this result can be explained by the 2-vinylpyridine monomer that provides greater stability to the material compared to the polymers synthesized with methacrylic acid. For all three MIPs, thermal stability up to around 300 °C was observed, thus confirming that these materials withstand critical working conditions.

The derivative of mass loss (dML) curves are presented in Fig. 6. It is observed that the thermal degradations take place in one or two steps for the polymeric materials. For ME-DCF-01, the main thermal event starts around 200 °C, has the maximum degradation rate at 363 °C with a weight loss of 35%, and stops around 460 °C. MB-NPX-03 polymer has a maximum degradation rate at 345 °C with a weight loss of 42%; this single thermal degradation step starts around 250 °C and ends around 440 °C. Finally, for MB-IBP-04, thermal degradation occurs in two steps. The main step starts around 250 °C, having a maximum degradation rate at 319 °C with a weight loss of 32%, and ends around 440 °C. The second step has a maximum degradation rate of around 400 °C.

The MIP of DCF and NPX (ME-DCF-01 and MB-NPX-03, respectively) exhibit very close maximum degradation rates because both polymers were synthesized with MAA as the monomer. This compound in a temperature range of 270 °C to 450 °C decomposes by dehydration of the acid groups forming anhydrides, which then decompose by decarboxylation (Cervantes-Uc et al. 2006; Dima et al. 2012). For MB-IBP-04, the weight loss in the 300 °C to 400 °C regions is mainly attributed to cleavages in the crosslinker-monomer bonds and thermooxidative degradation of the vinylpyridine chain, respectively (Jaymand 2011; Wu et al. 2003).

Fourier transform infrared spectroscopy (FT-IR)

The FT-IR spectra for DCF, NIP-E1, and ME-DCF-01 are observed in Fig. 7a. Two characteristic bands are seen at 1573 and 1397 cm^{-1}, related to C = OCOO- stretching vibrations and O-CO-CH3 bending vibrations; respectively, these are attributed to the functional groups' diclofenac. The broad bands at 3401 and 3235 cm^{-1} are attributed to the N–H bond-related bending and stretching vibrations, which may be due to template and polymer matrix effects. The sawtooth peaks in 700–800 cm^{-1} can be attributed to aromatic substitutions at positions 1, 2, and 3 of the DCF. Therefore, all these bands are associated with the DCF molecule, confirming that the template molecule was imprinted on the MIP.

Figure 7b shows the FT-IR spectra of the NPX, NIP-B3, and MB-NPX-03 samples. The peaks confirm the presence of the template molecule (NPX) in the MIP at 1586, 1370, and 800–900 cm^{-1}, corresponding to the vibrations of the aromatic C=C, aromatic $-CH_3$, and adjacent aromatic 1,2-hydrogen bonds, respectively. The similarity in peaks between MIP and NIP spectra of NPX at 2983 and 2998 cm^{-1} (CH_3 bond vibration), 1723 cm^{-1} (corresponding to C=O bond), 1631 and 1625 cm^{-1} (C=C bond stretching vibration), and 1450 and 1454 cm^{-1} (C-O bond vibration) is attributed to the functional groups of the polymeric matrix, which is the same for MIP and NIP.

The spectra of IBP, NIP-B4, and MB-IBP-04 are shown in Fig. 7c; the characteristic bands of IBP corresponding

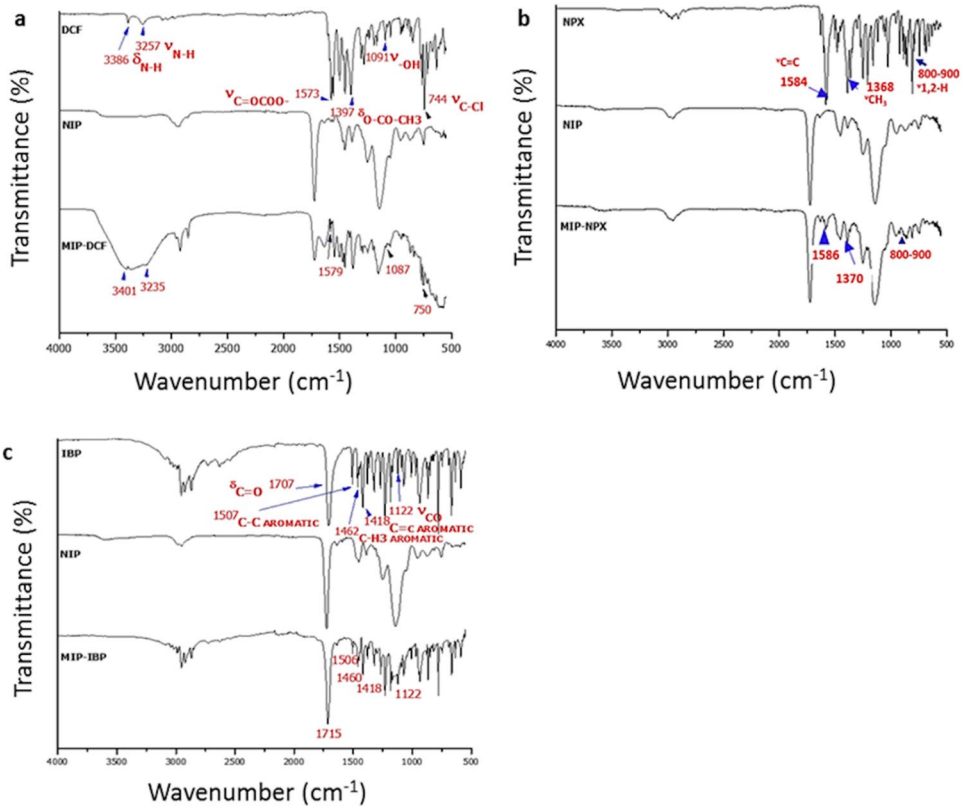

Fig. 7 FT-IR spectra. **a** ME-DCF-01/NIP-E1/DCF. **b** MB-NPC-03/NIP-B3/NPX. **c** MB-IBP-04/NIP-B4/IBP

to the bending vibrational modes of C = O groups (1707 cm^{-1}), stretching vibrations of C-O (1122 cm^{-1}), and vibrations of C–C, C-H_3, and C = C aromatic bond (1507, 1462, and 1418 cm^{-1}, respectively) can be observed. In addition, the MIP spectrum of IBP showed all the above-mentioned characteristic vibrational bands of IBP, indicating the presence of the drug in the MIP structure.

Specific area and pore diameter

The specific area and average pore diameter of MIPs and NIPs were calculated using the BET and BJH methods. Table 2 shows the obtained values, where specific area values in the range of 111 to 410 $m^2\ g^{-1}$ are observed, indicating that both MIPs and NIPs are materials with high porosity. In addition, the obtained pore diameters evidenced that all the materials are mesoporous. The specific area of MIPs is larger than that of NIPs; this result is explained by the effectiveness of stencil printing (Tabaraki and Sadeghinejad 2020). In addition, it was found that the mass polymerization method improves pore formation and specific area since values of the specific area and pore volume are higher than the values obtained from the polymers obtained by emulsion.

It has been reported that in polymerizations, toluene is a good pore former in the presence of MAA and EDGMA (Sellergren and Shea 1993). These results were confirmed by Renkecz et al. (2014), where they observed a difference in pore size of up to fourfold of DCF MIPs synthesized with toluene with respect to chloroform (Renkecz et al. 2014). On the other hand, when comparing the results of surface area for NPX (S_{BET}: 17 m^2g^{-1}) and DFC (S_{BET}: 24 m^2g^{-1}) MIPs of this author, we observed that our MIPs present from 4.6 to 17 times greater surface area with respect to their MIPs; it should be noted that they used 4-vinylpyridine as monomer.

Point of zero charges (PZC) of the adsorbent

The surface charge of material in an aqueous solution is generated from interactions between ions in solution (H + and HO −) and the surface functional groups of the adsorbent.

Table 2 Textural properties of MIPs and NIPs

Parameters	ME-DCF-01	MB-NPX-03	MB-IBP-04	NIP-E1	NIP-B3	NIP-B4
S_{BET} (m^2/g)	111	410	372	106	402	318
V_P (cm^3/g)	0.491	0.922	1.234	0.791	1.452	0.601
D_p (nm)	14.183	12.714	17.711	15.231	19.858	11.141

Surface charge and point of zero charges (PZC) are essential features in adsorbent surface science and play a key role in the adsorption process. The surface charge of the adsorbent with acidic and basic groups is highly dependent on the pH of the surrounding solution, and the interaction between the adsorbent surface sites and the electrolyte species determines the PZC (Madrakian et al. 2013).

Depending on the pH of the solution, the surface-active sites of an adsorbent may undergo protonation or deprotonation, and thus, a charged surface will be formed. Figure 8a shows the potentiometric curves for the blank and the solution with the ME-DCF-01 polymer. It is observed that the curves intersect at a pH value of 3.35, indicating that the PZC for MIP is acidic, similarly observed for NIP-E1, where the curves intersect at 3.15 (Fig. 8b). Concerning the polymers MB-NPX-03 and NIP-B3, acidic PZC of 3.18 and 3.12 were obtained, respectively. These results can be attributed to the monomer used in the synthesis of the polymers since they were all synthesized with methacrylic acid (weak acid pKa 4.7).

On the contrary, for the polymers MB-IBP-04 and NIP-B4, the PZC was 8.89 and 7.98, respectively, so the PZC is basic. The above is attributed to 2-vinylpyridine, which is a weak base of pKa 4.9.

Adsorption isotherms and kinetics

The obtained kinetic data were analyzed by the pseudo-first-order (PFO) and pseudo-second-order (PSO) models. Table 3 shows the kinetic adsorption parameters of DCF, NPX, and IBP on the corresponding MIP and NIP with an initial concentration of 10 mg L^{-1}. It is observed that all the tested polymers were best fit to the PSO model due to the R^2 value close to 1. These results could indicate that the target molecules are adsorbed on the binding sites via chemisorption bonds, which involve a chemical reaction or chemical-like force bonding between the functional groups of the adsorbent and the template. The best fit to the PSO model indicated that the adsorption mechanism could depend on both the adsorbate and the adsorbent, and the rate-limiting step is chemisorption involving valence forces through the exchange of electrons (Surikumaran et al. 2014).

For all MIPs and NIPs, adsorption increased rapidly in the first 20 min and reached equilibrium at 30 min. This type of polymeric adsorbent generally shows very fast equilibrium times, representing an excellent methodological advantage. With other adsorbents, the equilibrium time can take several days (Guo et al. 2018). On the other hand, the MIPs presented higher adsorption capacities compared to

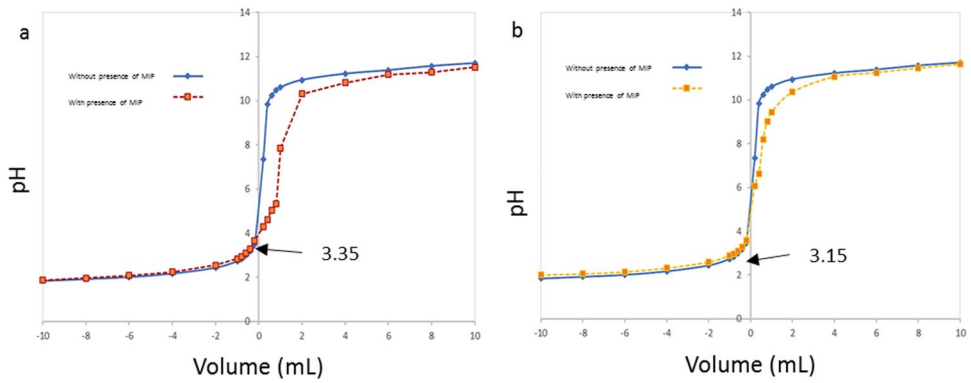

Fig. 8 Potentiometric curves. **a** Blank and solution with ME-DCF-01. **b** Blank and solution with NIP-E1

Table 3 Comparison of pseudo-first-order and pseudo-second-order kinetic parameters for MIPs and NIPs

MIP/NIP	$q_{e,exp}$ (mg g^{-1})	Pseudo-first-order			Pseudo-second-order		
		$q_{e,cal}$ (mg g^{-1})	k_1 (min^{-1})	R^2	$q_{e,cal}$ (mg g^{-1})	k_2 (g mg^{-1} min^{-1})	R^2
ME-DCF-01	0.491	0.429	0.0758	0.821	0.511	0.0965	0.996
NIP-E1	0.237	0.204	0.0585	0.901	0.218	0.0487	0.994
MB-NPX-01	0.481	0.469	0.0618	0.931	0.498	0.0847	0.998
NIP-B3	0.254	0.198	0.0129	0.811	0.258	0.0488	0.997
MB-IBP-04	0.496	0.473	0.0719	0.901	0.514	0.0898	0.993
NIP-B4	0.284	0.247	0.0351	0.901	0.264	0.0691	0.995

20 mg of MIP or NIP, initial concentration of 10 mg L^{-1}, pH 6, 24 °C

$q_{e,exp}$ and $q_{e,cal}$ are the amount of adsorbate (mg g^{-1}) on adsorbent at experimental and calculated equilibrium, respectively

k_1 and k_2 constants of the pseudo-first-order and pseudo-second-order model, respectively

R^2 correlation coefficient

the non-imprinted polymers. As shown in Fig. 9, for MB-IBP-04, q_e was 0.514 mg g^{-1}, exhibiting a higher adsorption capacity than NIP-B4 (0.264 mg g^{-1}) and obtaining faster adsorption due to the higher value of the k^2 constant. This phenomenon was observed for all 3 MIPs evaluated and their corresponding NIPs; thus, this confirms the positive effect of molecular imprinting on the adsorption capacity.

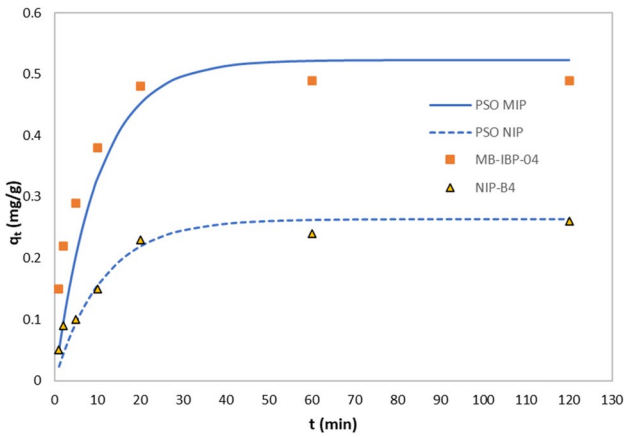

Fig. 9 Pseudo-second-order kinetic models for MB-IBP-04 and NIP-B4 (20 mg MIP or NIP, initial concentration of 10 mg L^{-1}, pH 6, 24 °C)

The MIPs show similar adsorption mechanisms, due to similarities in adsorbent synthesis, both in terms of polymerization reagents and methodology, and to the physicochemical properties of the analytes, mainly the very close pKa of the 3 NSAIDs.

Equilibrium data were fitted to the Freundlich, Langmuir, and Redlich-Peterson models. The best fit of the isotherm models was chosen by the value of the correlation coefficient (R^2) closest to 1. The constants of the adsorption isotherms at different pHs for the MIPs/NIPs are shown in Table 4. The polymers ME-DCF-01 and MB-NPX-03 fitted the Langmuir model best at pH 6 and 24 °C (R^2 = 09,846 and 0.9896, respectively), which indicates that adsorption can occur in a monolayer and is considered a homogeneous surface with a specific number of binding sites where a molecule can be adsorbed. It should be noted that in ME-DCF-01 an R^2 value closer to 1 for the Redlich-Peterson model was obtained; however, because β equals 1, the isotherm is transformed to the Langmuir isotherm; therefore, the model is adequately described by the two isotherms mentioned. In comparison, the corresponding NIPs, NIP-E1 and NIP-B3, were better fitted to the Freundlich and Langmuir model, respectively.

The imprinted polymer MB-IBP-04 best fits the Freundlich model at pH 6 and 24 °C (R^2 = 0.9896), indicating that adsorption occurs in multilayer and the value of $n > 1$

Table 4 Adsorption isotherm constants for the MIPs/NIPs evaluated at different pH (20 mg MIP/NIP, 30 min contact, 1 mL solution, medium temperature 24 °C)

MIP/NIP	pH	Langmuir			Freundlich			Redlich-Peterson			
		q_m (mg g^{-1})	K (L mg^{-1})	R^2	k ($mg^{1-1/n}L^{1/n}/g$)	n	R^2	a (L g^{-1})	b (L $mg^{-1})^{\beta}$	β	R^2
ME-DCF-01	3	14.1	0.199	0.968	4.32	4.34	0.996	2.33	0.162	1	0.997
	6	13.6	0.0998	0.984	5.11	5.48	0.808	1.19	0.0872	1	0.986
	9	12.4	0.256	0.996	3.58	4.24	0.991	2.91	0.524	0.862	0.998
NIP-E1	3	5.06	0.0286	0.915	1.71	1.03	0.971	0.996	0.108	1	0.964
	6	4.70	0.00646	0.926	1.64	0.938	0.961	1.60	0.649	0.689	0.958
	9	3.42	0.0219	0.935	0.289	0.996	0.961	0.891	0.0982	0.894	0.932
MB-NPX-03	3	21.6	0.146	0.994	6.24	3.94	0.978	3.06	0.140	1	0.995
	6	12.6	0.0789	0.989	3.07	3.84	0.961	0.995	0.0789	1	0.989
	9	10.7	0.0083	0.991	0.681	2.12	0.980	0.126	0.0099	1	0.991
NIP-B3	3	4.53	0.0889	0.989	1.94	1.68	0.961	0.591	0.0196	1	0.971
	6	3.48	0.0712	0.982	0.875	1.12	0.981	1.66	0.0438	0.785	0.914
	9	2.98	0.0532	0.961	0.601	0.956	0.951	1.52	0.0349	0.811	0.983
MB-IBP-04	3	14.1	0.169	0.989	4.15	4.12	0.998	6.46	0.947	0.862	0.998
	6	16.5	0.0429	0.976	4.26	4.19	0.989	5.26	0.945	0.816	0.981
	9	13.2	0.0388	0.997	1.86	2.86	0.981	0.523	0.0395	1	0.997
NIP-B4	3	5.27	0.0617	0.961	2.71	1.91	0.941	2.06	0.0892	0.781	0.981
	6	5.13	0.0491	0.977	2.12	1.25	0.931	1.99	0.0913	0.864	0.905
	9	4.58	0.0547	0.953	1.98	1.04	0.951	0.891	0.0489	0.552	0.983

20 mg of MIP or NIP, 24 °C. q_m is the maximum amount of adsorbate (mg g^{-1}) on adsorbent at equilibrium. K is the Langmuir constant, k is the Freundlich constant, and n is the exponent of the Freundlich isotherm. a, b, and β are the constants of the R-P isotherm and R is the correlation coefficient

indicates a favorable adsorption condition in IBP MIP. This model describes that most of the surfaces are heterogeneous, and multiple sites are available for adsorption. The obtained values of *k* indicate that the molecules are adsorbed with an intensity characteristic for a chemisorption process. As for NIP-B4, it fitted best to the Langmuir isotherm, following the characteristics mentioned above for this model.

When analyzing the influence of pH in the medium, it was found that the adsorption capacity of the MIPs against each NSAID is higher in the acidic region than in the alkaline region. As can be observed in Fig. 10a, b with the imprinted polymers, adsorption at pH 3 and 6 has a higher removal of DCF and NPX compared to adsorption at pH 9. This is because both MIPs at pH 3 have a surface charge close to zero since the PZC is 3.35 for the DCF MIP and 3.18 for the NPX MIP. Furthermore, at pH 6, good removal of each template molecule is obtained because the surface charge, although negative, is very low, so there is no noticeable repulsion between the adsorbent and the adsorbate.

In addition, because the pKa of DCF is 4.2 and that of NPX is 4.3, these pollutants exist mainly as their conjugate base forms at basic pH (Fig. 10). Consequently, the electrostatic repulsion is lower at acidic pH in solution so that, at pH 9, the adsorption of both analytes decays. These results suggest that attractive hydrogen bonds and other interactions promote adsorption.

For MB-IBP-04, higher IBP removal efficiency was obtained in a pH range of 3 to 6 (Fig. 10c). This is because the surface charge of the MIP is almost neutral in that pH range; in addition, the pKa for 2-VP is 4.9, which promotes Van der Waals force interactions between the IBP molecules and the adsorbent since at pH < 4.9 IBP is in its protonated form. The removal efficiency decreased at pH 9 due to repulsive interactions between negative IBP molecules and the MIP surface. The results obtained in the isotherms by the influence of the pH of the medium suggest that the main interactions between DFC/NPX/IBP and each MIP or NIP were mainly related by electrostatic or Van der Waals forces. A good imprinting effect was also demonstrated for MIP having a higher adsorption efficiency than NIP over the whole pH range evaluated.

A comparison of the values obtained with other MIPs synthesized with different methods was performed; it is observed that the retention percentages are similar in all the studies (Table 5). In the study carried out by Madikizela and Chimuka (2016a), a MIP was designed by the bulk method with NPX, IBP, and DCF as templates, 2-vinylpiridine as functional monomer, and EDGMA as crosslinker.

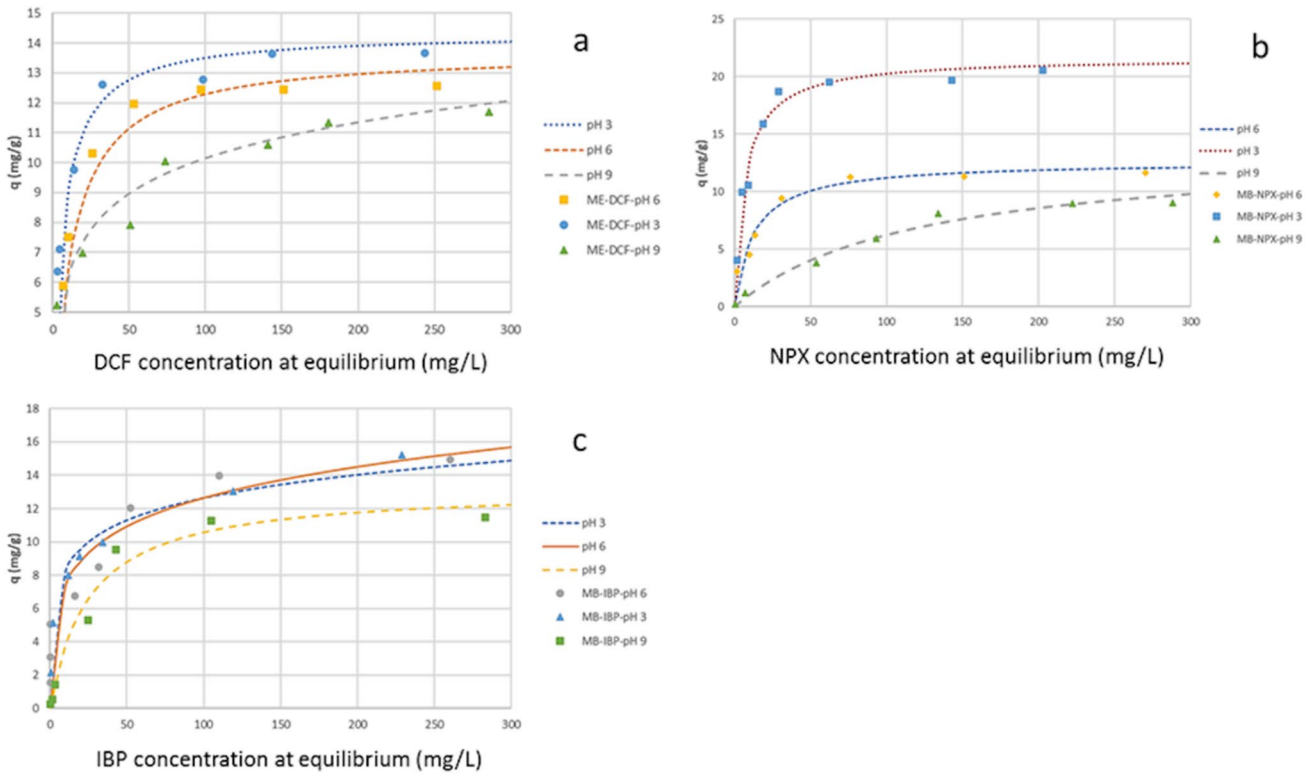

Fig. 10 Effect of pH on the best-fit adsorption isotherms for each NSAID on the corresponding MIP at 24 °C. **a** Redlich-Peterson isotherms for ME-DCF-01. **b** Langmuir isotherms for MB-NPX-03. **c** Redlich-Peterson isotherms for MB-IBP-04. 20 mg of MIP or NIP, 30 min contact, 1 mL solution, medium temperature 24 °C

In the study, the MIP fits the Langmuir model better, and equivalent maximum adsorption capacities were obtained compared to our material.

Imprinting factor and selectivity of MIPs and NIPs

To evaluate the selectivity of the imprinted polymers against the molecule for which it was designed, the imprinting factor (IF) was calculated for each MIP; these values are presented in Table 6. It was observed that the polymer ME-DCF-01 and MB-NPX-03 with methacrylic acid monomer showed a high adsorption capacity (q_e) to adsorb DCF and NPX and low for IBP; similarly, the K_{MIP} partition coefficient values are higher for DCF and NPX than for IBP; these results were similar in the study of Dai et al. (2013), where they indicate the similarity of extraction between carbamazepine and DCF; this study explains the imprinting between the template molecule with the monomer. Carbamazepine and DCF have a benzene ring and carboxylic group that could have printed similarly with the 2-vinylpyridine monomer used in this study, which affected the recognition and resulted in high extraction capacities but low selectivity (Dai et al. 2013). Although IBP has a similar structure to DCF and NPX, the extraction capacity is lower than DCF and NPX, indicating that the memory of the specific functional group plays an important role in conformation memory (An et al. 2008). Thus, MIP recognition was dominated not only by the size of the molecule but also by the distribution of the functional groups themselves.

The imprinted polymer MB-NPX-03 obtained a higher IF towards NPX; however, the retention rate towards DCF and IBP is high, 97.6% and 89.8%, respectively. This shows that the polymers ME-DCF-01 and MB-NPX-03 can adsorb in high percentages the 3 studied NSAIDs, since the molecules are homologous and have very similar physicochemical properties, such as pKa (4–5), so the mole fraction of protonated species and conjugated bases will be practically the same at any pH in the medium. In contrast, MB-IBP-04 obtained a higher IF towards IBP compared to those obtained towards DCF and NPX, so this MIP is selective towards its template molecule; possibly, the success in molecular imprinting in MIP is due to the simpler and less sterically hindered structure of IBP. This result was similar to that obtained by Madikizela and Chimuka, obtaining a percentage of recovery between 85 and 103% for the same NSAIDs evaluated in this study, synthesizing a polymer by bulking using 2-VP as

Table 5 Comparative study of MIPs synthesized for NSAID adsorption

Template/polymerization approach	Monomer/crosslinker/porogen	Change conditions	Retention rate	Isotherm parameters	Analytical method	References
DCF (emulsion) and NPX (bulk)	Methacrylic acid EDGMA Toluene	20 mg MIP 1 mg L^{-1} pH 6	> 98	Langmuir: q_m 13.56 and 12.60 mg g^{-1}	HPLC–DAD	This study
IBP (bulk)	2-Vinylpyridine EDGMA Toluene	20 mg MIP 1 mg L^{-1} pH 6	99	Freundlich $k = 4.26$ mg$^{1-1/n}$L$^{1/n}$/g $n = 4.1$	HPLC–DAD	This study
DCF (co-precipitation)	4-Vinylpyridine EDGMA Acetonitrile	50 mg MIP	100	–	HPLC	(Mohiuddin et al. 2020)
DCF (bulk)	Methacrylic acid EDGMA Acetonitrile	5 mg MIP 10^{-4} M	90	–	GC–MS	(Cantarella et al. 2019)
DCF/NPX/IBP (bulk)	2-Vinylpyridine EDGMA Acetonitrile/toluene	50 mg MIP 20 mg L^{-1} pH 4.6	DCF 99 NPX 85 IBP 89	Langmuir $Q_{m\,(NPX)} = 4.474$ mg g^{-1} $Q_{m\,(DCF)} = 5.453$ mg g^{-1}	HPLC	(Madikizela and Chimuka 2017)
NPX (chiral MIP)	4-Vinylpyridine EDGMA Methanol/dimethyl sulfoxide	–	84	–	HPLC–DAD	(Liu et al. 2020)
DCF (co-precipitation)	Methacrylic acid EDGMA	100 mg MIP pH 5	92	SIPS $Q_m = 108.08$ mg g^{-1} n = 1.515	HPLC	(Zheng et al. 2018)
IBP (bulk)	4-Vinylpyridine EDGMA Acetonitrile	200 mg MIP 20 µg/mL	83	–	HPLC	(Farrington and Regan 2007)

DCF diclofenac, *NPX* naproxen, *IBP* ibuprofen, *EDGMA* ethylene glycol dimethacrylate

Table 6 Partition coefficients and imprinting factors of DCF, NPX, and IBP on the corresponding MIP and NIP. C_0 and C mg L^{-1}, q mg g^{-1}, and K_{MIP} and K_{NIP} mL g^{-1}

Template	ME-DCF-01/NIP-E1									
	C_0 (mg L^{-1})*	C (mg L^{-1})*	q_e (mg g^{-1})*	$\%R$ *	K_{MIP} (mL g^{-1}) *	C_0 (mg L^{-1})**	C (mg L^{-1})**	q_e (mg g^{-1})**	$\%R$ **	K_{NIP} (mL g^{-1})**	IF
DCF	2.0	0.033	0.0984	98.33	2980.3	2.0	0.444	0.0778	77.80	175.22	17.01
NPX	2.0	0.040	0.0980	97.98	2450.0	2.0	0.506	0.0747	74.68	147.63	16.60
IBP	2.0	0.108	0.0946	94.59	875.93	2.0	0.676	0.0662	66.19	97.929	8.940
Template	MB-NPX-03/NIP-B3										
DCF	2.0	0.048	0.0976	97.58	2033.3	2.0	0.566	0.0717	71.70	126.68	16.05
NPX	2.0	0.041	0.0980	97.94	2389.0	2.0	0.562	0.0719	71.89	127.94	18.67
IBP	2.0	0.203	0.0899	89.83	442.61	2.0	0.600	0.0700	69.97	116.67	3.790
Template	MB-IBP-04/NIP-B4										
DCF	2.0	0.139	0.0931	93.06	669.42	2.0	0.545	0.0728	72.78	133.49	5.010
NPX	2.0	0.208	0.0896	89.61	430.77	2.0	0.404	0.0798	79.80	197.52	2.180
IBP	2.0	0.045	0.0978	97.77	2172.2	2.0	0.422	0.0789	78.88	186.97	11.62

DCF diclofenac, *NPX* naproxen, *IBP* ibuprofen, q_e amounts of adsorbate bound, $\%R$ percentage retention, K_{MIP} partition coefficients of MIP, K_{NIP} partition coefficients of MIP, *IF* imprinting factor

*MIP, **NIP

monomer and the 3 NSAIDs in combination as a template (Madikizela and Chimuka 2016b). On the other hand, an interference assay was performed with sulfamethoxazole and ciprofloxacin, and retention of less than 30% of these compounds was observed, indicating that the MIPs of NSAIDs are specific because they are similar molecules.

Additionally, the values of partition coefficients determined for MIPs (K_{MIP}) and NIPs (K_{NIP}) and shown in Table 6 ranged from 430.77 to 2980.3 and from 97.93 to 197.52 mL g^{-1}, respectively. According to Parra-Marfíl et al. (2020), partition coefficient values higher than mL g^{-1} are considered adequate, indicating that MIPs are highly affine to DCF, NPX, and IBP. The $\%R$ or q_e values give a measure of the adsorbate removed, while the partition coefficient is a direct measurement of the affinity of the adsorbent for adsorbate under the conditions it is tested (Parra-Marfíl et al. 2020).

Pilot study: concentrations of NSAIDs in wastewater from the city of San Luis Potosí, Mexico

A pilot study was conducted using the characterized MIPs in wastewater samples from San Luis Potosí city to evaluate the feasibility of applying our technology. Table 7 shows the average concentrations of each NSAID found in raw wastewater and fortified water samples at 1 mg L^{-1}. With the use of the imprinted polymers, the following amounts of each template molecule were concentrated: with ME-DCF-01 0.642 mg $L^{-1} \pm 0.068$ mg L^{-1}, with MB-NPX-03 0.987 mg $L^{-1} \pm 0.184$ mg L^{-1}, and with MB-IBP-04 0.403 mg $L^{-1} \pm 0.071$ mg L^{-1}. Figure 11 shows examples of the chromatograms in fortified water and problem sample (wastewater); it is observed that the 3 MIPs present excellent retention of NSAIDs, but we consider that the most important result in this section was the evaluation of the fortified water, demonstrating the high pre-concentration of NSAIDs, but also the decrease of the matrix effect in a complex sample.

Higher concentrations were obtained for the template molecules using their corresponding MIP, while extraction of molecules different from the MIP template obtained lower concentrations; this indicates that the evaluation of NSAIDs should focus on the corresponding MIP for each target molecule.

In our country, there are no regulations that determine the concentrations and discharges of pharmaceuticals in water; in addition, these types of compounds are not eliminated in their entirety in the conventional wastewater treatment process. The NSAIDs evaluated in the present study are the most consumed and therefore discarded worldwide; now, in the context of COVID-19, the use of antipyretics and anti-inflammatory drugs increased up to 27% (O'Flynn et al. 2021), as well as their presence in wastewater treatment plants (Yan et al. 2021). From the pharmacological point of view, NSAIDs are primarily designed to carry out

Table 7 Concentration of DCF, NPX, and IBP found in wastewater and fortified water

MIP/SAMPLE	[DCF] mg L^{-1}	SD_{DCF}	[NPX] mg L^{-1}	SD_{NPX}	[IBP] mg L^{-1}	SD_{IBP}
ME-DCF-01 wastewater	0.6424	0.06825	0.7467	0.06215	0.2105	0.1891
ME-DCF-01 fortified water	0.9752	0.1638	0.9771	0.03522	0.9145	0.08091
MB-NPX-03 wastewater	0.3968	0.1065	0.9875	0.1837	0.1861	0.06036
MB-NPX-03 fortified water	1.0238	0.01908	1.0203	0.03306	1.0060	0.03706
MB-IBP-04 wastewater	0.8485	0.07198	0.0307	0.02662	0.4031	0.07080
MB-IBP-04 fortified water	0.9829	0.03685	0.9748	0.08705	1.0326	0.05509

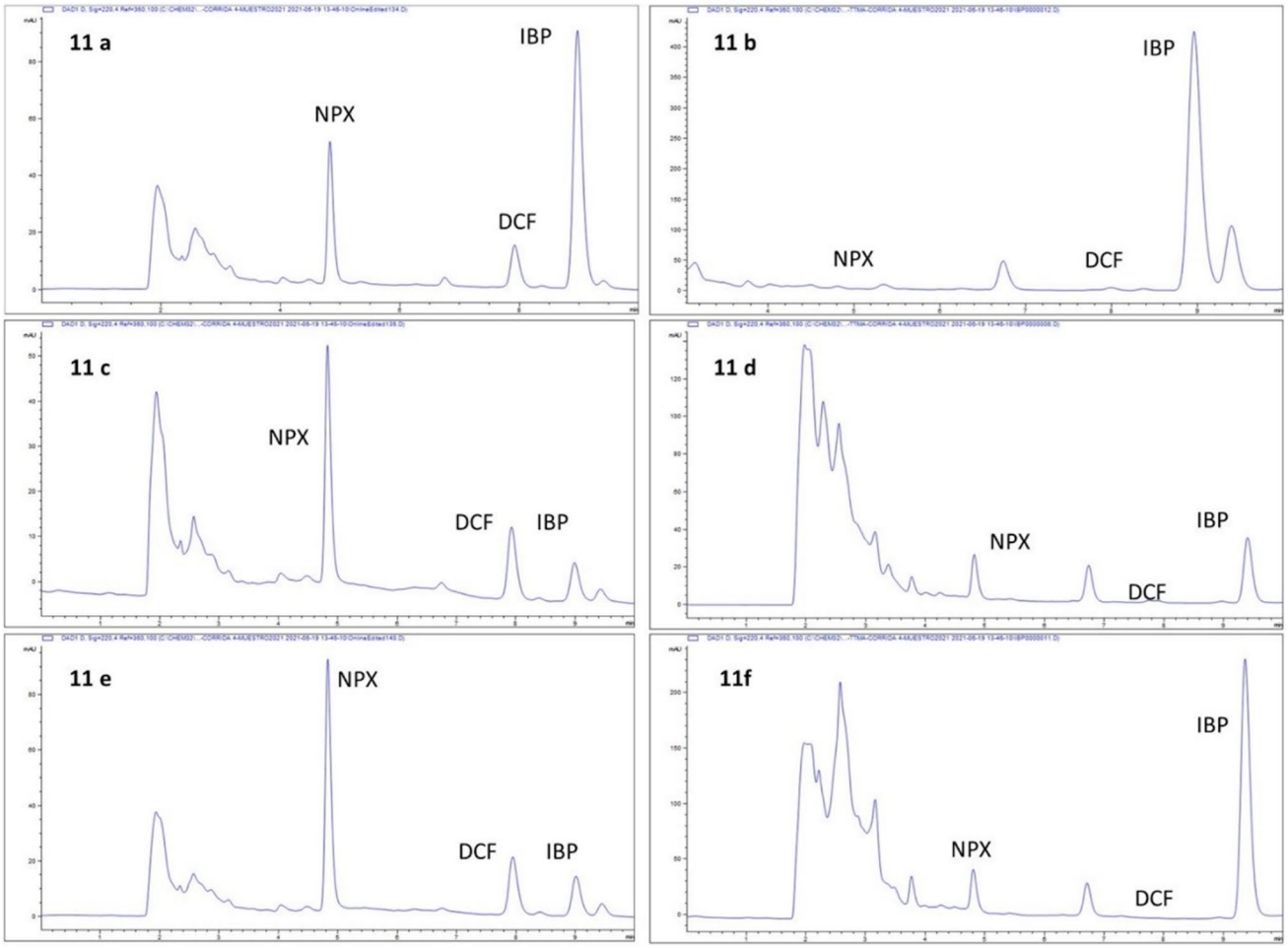

Fig. 11 Chromatograms of samples of fortified water (1 mg L^{-1}) and wastewater. **a** MB-IBP-04/IBP-fortified water. **b** MB-IBP-04/IBP-wastewater. **c** ME-DCF-01/DCF-fortified water. **d** ME-DCF-01/DCF-wastewater. **e** MB-NPX-03/NPX-fortified water. **f** MB-NPX-03/NPX-wastewater

physiological processes and resist inactivation before exerting the therapeutic effect for which they were developed. These properties are also responsible for their low biodegradability and potential toxic effects in aquatic and terrestrial ecosystems, which is increased by the continuous introduction into these environments (Joachim et al. 2021; Wang et al. 2021).

To compare NSAID concentrations in the study, research conducted in Mexico, where the concentrations of these compounds have been determined in wastewater treatment plants, were evaluated. Rivera et al. evaluated the concentration of different drugs in the influent and effluent of a wastewater treatment plant in Cuernavaca, Morelos, finding in the influent a concentration of DCF of 0.0023 mg L^{-1}, 0.0026 mg L^{-1} of NPX, and 0.0019 mg L^{-1} of IBP, while in the effluent they reported a concentration of DCF of 0.002 mg L^{-1}, 0.00026 mg L^{-1} of NPX, and no IBP was detected (Rivera-Jaimes et al. 2018). In another study, 12

effluents from three wastewater treatment plants in the Metropolitan Zone of the Valley of Mexico were analyzed: University City (CU), Coyoacán, and Cerro de la Estrella. For IBP, the concentration in the effluents ranged from 0.0002 to 0.0028 mg L^{-1}. NPX was the analyte quantified in the highest concentration in the three treatment plants; in the effluents, its concentration ranged from 0.0028 to 0.054 mg L^{-1} (Peña-Álvarez and Castillo-Alanís 2015).

In developing countries, monitoring of the pollutants in this study is not routinely performed; therefore, there are no regulations that establish permissible limits in environmental matrices that protect human and ecosystem health (Vargas-Berrones et al. 2020). (Vargas-Berrones et al. 2020). This may be due to the lack of availability of highly sensitive instrumentation such as liquid chromatography coupled to time-of-flight and quadrupole mass spectrometry and lack of access to purchase or/and maintain the operating costs associated with these technologies. To address this challenge, research must focus on the development of preparative techniques that can improve the sensitivity of laboratory instruments. We demonstrated that the synthesized materials show similar retention and reproducibility values to various studies; however, no significant applications have been demonstrated in wastewater in developing countries. Thus, research in the environmental area is of great relevance in our country, with the purpose of providing information to the authorities for the establishment of pertinent regulations for the protection of the environment and human health.

Conclusion

A highly selective and efficient material was developed for the quantification of DCF, NPX, and IBP in wastewater samples. 10 min of contact with the solution and 20 mg of MIP were sufficient to obtain high percentages of DCF, NPX, and IBP recovery of 98.3, 99, and 97.7% respectively. The three evaluated MIPs exhibited thermal stability up to 300 °C, and it was observed that 2-VP confers greater stability to the material; in addition, we obtained mesoporous materials with a pore size between 10 and 20 nm. Additionally, it was observed that the material charge is influenced by the functional monomer; in the case of the DCF and NPX MIPs, the PZC value was 3.35 and 3.15 using the MAA monomer, and for the IBP MIP, it was 9.89 using 2-VP; this is related to the release of the compounds from the material observing that at pH 3 a higher release occurs regarding pH 9 for DFC and NPX; in the case of IBP, higher IBP removal efficiency was obtained in a pH range of 3 to 6; this is because the surface charge of the MIP is almost neutral in that pH range; in addition, the pKa for 2-VP is 4.9, which promotes Van der Waals force interactions between the IBP molecules and the adsorbent since at pH < 4.9 ibuprofen is in its protonated form.

Higher concentrations were obtained for the template molecules using their corresponding MIP, while extraction of molecules different from the MIP template obtained lower concentrations; this indicates that the evaluation of NSAIDs should focus on the corresponding MIP for each target molecule. Finally, the MIPs were used to determine the NSAIDs understudy in San Luis Potosí, México, wastewater, finding concentrations of 0.642, 0.985, and 0.403 mg L^{-1} for DCF, NPX, and IBP, respectively. In our country, there are no regulations that determine the concentrations and discharges of pharmaceuticals in water; in addition, these types of compounds are not eliminated in their entirety in the conventional wastewater treatment process. The NSAIDs evaluated in the present study are the most consumed and therefore discarded worldwide; now, in the context of COVID-19, the use of antipyretics and anti-inflammatory drugs increased up to 27% (O'Flynn et al. 2021), as well as their presence in wastewater treatment plants (Yan et al. 2021). Drug extraction using MIPs can effectively replace traditional extraction methodologies due to the multiple advantages that they present, such as reusability, low cost, and stability. Consequently, molecularly imprinted polymers could be an alternative for the determination of this type of contaminants in complex environmental matrices.

Author contribution JMM: conceptualization, sampling, analytical methods, writing, and editing; LDLM: conceptualization and analytical methods, writing, and editing; VGR: conceptualization and funding; SVL: conceptualization and analytical methods; ROP: analytical methods; NAMC: sampling and conceptualization; EPO: conceptualization, sampling, writing, and editing; IRT: conceptualization and sampling; RRF: conceptualization, analytical methods, writing and editing, and funding.

Funding The authors acknowledge grants and fellowships from the National Council on Science and Technology-Sectoral Research Fund for Education Basic-Science #A1-S-28176.

Data availability Not applicable.

Declarations

Ethics approval and consent to participate Not applicable.

Consent for publication.
Not applicable.

Competing interests The authors declare no competing interests.

References

An F, Gao B, Feng X (2008) Adsorption and recognizing ability of molecular imprinted polymer MIP-PEI/SiO2 towards phenol. J Hazard Mater 157:286–292

Bartoskova M, Dobsikova R, Stancova V, Zivna D, Blahova J, Marsalek P et al (2013) Evaluation of ibuprofen toxicity for zebrafish (Danio

rerio) targeting on selected biomarkers of oxidative stress. Neuro Endocrinol Lett 34(2):102–108
Bonnefille B, Gomez E, Courant F, Escande A, Fenet H (2018) Diclofenac in the marine environment: a review of its occurrence and effects. Mar Pollut Bull 131:496–506
Cantarella M, Carroccio SC, Dattilo S, Avolio R, Castaldo R, Puglisi C, Privitera V (2019) Molecularly imprinted polymer for selective adsorption of diclofenac from contaminated water. Chem Eng J 367:180–188
Cervantes-Uc J, Cauich-Rodríguez J, Vázquez-Torres H, Licea-Claveríe A (2006) TGA/FTIR study on thermal degradation of polymethacrylates containing carboxylic groups. Polym Degrad Stab 91:3312–3321
Chen H, Son S, Zhang F, Yan J, Li Y, Ding H, Ding L (2015) Rapid preparation of molecularly imprinted polymers by microwave-assisted emulsion polymerization for the extraction of florfenicol in milk. J Chromatogr B 983–984:32–38
Dai C-m, Zhang J, Zhang Y-l, Zhou X-f, Duan Y-p, Liu S-g (2013) Removal of carbamazepine and clofibric acid from water using double templates–molecularly imprinted polymers. Environ Sci Pollut Res 20:5492–5501
de Leon-Martinez LD, Melendez-Marmolejo J, Vargas-Berrones K, Flores-Ramirez R (2020) Synthesis and evaluation of molecularly imprinted polymers for the determination of di(2-ethylhexyl) phthalate (DEHP) in water samples. Bull Environ Contam Toxicol 105:806–812
Diaz de León-Martínez L, Rodríguez-Aguilar M, Ocampo-Pérez R, Gutiérrez-Hernández JM, Díaz-Barriga F, Batres-Esquivel L, Flores-Ramírez R (2018) Synthesis and evaluation of a molecularly imprinted polymer for the determination of metronidazole in water samples. Bulletin of Environmental Contamination and Toxicology 100(3):395–401
Dima S-O, Sarbu A, Dobre T, Purcar V, Nicolae C-A (2012) Diosgenin selective molecularly imprinted polymers with acrylonitrile-methacrylic acid matrix. Materiale Plastice 49:106–113
Eslami A, Amini MM, Yazdanbakhsh AR, Rastkari N, Mohseni-Bandpei A, Nasseri S, Piroti E, Asadi A (2015) Occurrence of non-steroidal anti-inflammatory drugs in Tehran source water, municipal and hospital wastewaters, and their ecotoxicological risk assessment. Environ Monit Assess 187:734
Farrington K, Regan F (2007) Investigation of the nature of MIP recognition: the development and characterisation of a MIP for Ibuprofen. Biosens Bioelectron 22:1138–1146
Gani KM, Hlongwa N, Abunama T, Kumari S, Bux F (2021) Emerging contaminants in South African water environment- a critical review of their occurrence, sources and ecotoxicological risks. Chemosphere 269:128737
Gómez-Oliván LM, Galar-Martínez M, García-Medina S, Valdés-Alanís A, Islas-Flores H, Neri-Cruz N (2014) Genotoxic response and oxidative stress induced by diclofenac, ibuprofen and naproxen in Daphnia magna. Drug and Chemical Toxicology 37(4):391–399
Guo P, Yuan X, Zhang J, Wang B, Sun X, Chen X, Zhao L (2018) Dummy-surface molecularly imprinted polymers as a sorbent of micro-solid-phase extraction combined with dispersive liquid–liquid microextraction for determination of five 2-phenylpropionic acid NSAIDs in aquatic environmental samples. Anal Bioanal Chem 410:373–389
Islas-Flores H, Manuel Gómez-Oliván L, Galar-Martínez M, Michelle Sánchez-Ocampo E, SanJuan-Reyes N, Ortíz-Reynoso M, Dublán-García O (2017) Cyto-genotoxicity and oxidative stress in common carp (Cyprinus carpio) exposed to a mixture of ibuprofen and diclofenac. Environ Toxicol 32:1637–1650
Jaymand M (2011) Synthesis and characterization of novel type poly (4-chloromethyl styrene-grft-4-vinylpyridine)/TiO_2 nanocomposite via nitroxide-mediated radical polymerization. Polymer 52:4760–4769
Joachim S, Beaudouin R, Daniele G, Geffard A, Bado-Nilles A, Tebby C, Palluel O, Dedourge-Geffard O, Fieu M, Bonnard M (2021) Effects of diclofenac on sentinel species and aquatic communities in semi-natural conditions. Ecotoxicol Environ Saf 211:111812
Kot-Wasik A, Dębska J, Namieśnik J (2007) Analytical techniques in studies of the environmental fate of pharmaceuticals and personal-care products. TrAC Trends in Analytical Chemistry 26(6):557–568
Kuzin IA, Loskutov AI (1996) USSR. J Appl Chem 39:85
Liu Y, Liu Y, Liu Z, Zhao X, Wei J, Liu H, Si X, Xu Z, Cai Z (2020) Chiral molecularly imprinted polymeric stir bar sorptive extraction for naproxen enantiomer detection in PPCPs. J Hazard Mater 392:122251
Madikizela LM, Chimuka L (2016a) Synthesis, adsorption and selectivity studies of a polymer imprinted with naproxen, ibuprofen and diclofenac. J Environ Chem Eng 4:4029–4037
Madikizela LM, Chimuka L (2016b) Determination of ibuprofen, naproxen and diclofenac in aqueous samples using a multi-template molecularly imprinted polymer as selective adsorbent for solid-phase extraction. J Pharm Biomed Anal 128:210–215
Madikizela LM, Chimuka L (2017) Occurrence of naproxen, ibuprofen, and diclofenac residues in wastewater and river water of KwaZulu-Natal Province in South Africa. Environmental Monitoring and Assessment 189(7):1–12
Madikizela LM, Ncube S (2021) Occurrence and ecotoxicological risk assessment of non-steroidal anti-inflammatory drugs in South African aquatic environment: what is known and the missing information? Chemosphere 280:130688
Madikizela LM, Tavengwa NT, Chimuka L (2018) Applications of molecularly imprinted polymers for solid-phase extraction of non-steroidal anti-inflammatory drugs and analgesics from environmental waters and biological samples. J Pharm Biomed Anal 147:624–633
Madrakian T, Ahmadi M, Afkhami A, Soleimani M (2013) Selective solid-phase extraction of naproxen drug from human urine samples using molecularly imprinted polymer-coated magnetic multi-walled carbon nanotubes prior to its spectrofluorometric determination. Analyst 138:4542–4549
Mohiuddin I, Grover A, Aulakh JS, Lee S-S, Malik AK, Kim K-H (2020) Porous molecularly-imprinted polymer for detecting diclofenac in aqueous pharmaceutical compounds. Chem Eng J 382:1230023
O'Flynn D, Lawler J, Yusuf A, Parle-McDermott A, Harold D, Mc Cloughlin T, Holland L, Regan F, White B (2021) A review of pharmaceutical occurrence and pathways in the aquatic environment in the context of a changing climate and the COVID-19 pandemic. Anal Methods 13:575–594
Paíga P et al (2015) Development of a SPE–UHPLC–MS/MS methodology for the determination of non-steroidal anti-inflammatory and analgesic pharmaceuticals in seawater. Journal of Pharmaceutical and Biomedical Analysis 106:61–70
Parida VK, Saidulu D, Majumder A, Srivastava A, Gupta B, Gupta AK (2021) Emerging contaminants in wastewater: a critical review on occurrence, existing legislations, risk assessment, and sustainable treatment alternatives. J Environ Chem Eng 9:105966
Parolini M (2020) Toxicity of the non-steroidal anti-inflammatory drugs (NSAIDs) acetylsalicylic acid, paracetamol, diclofenac, ibuprofen and naproxen towards freshwater invertebrates: a review. Sci Total Environ 740:140043
Parra-Marfíl A, Ocampo-Pérez R, Collins-Martínez VH, Flores-Vélez LM, Gonzalez-Garcia R, Medellín-Castillo NA, Labrada-Delgado GJ (2020) Synthesis and characterization of hydrochar from industrial Capsicum annuum seeds and its application for

the adsorptive removal of methylene blue from water. Environ Res 184:109334

Peña-Álvarez A, Castillo-Alanís A (2015) Identificación y cuantificación de contaminantes emergentes en aguas residuales por microextracción en fase sólida-cromatografía de gases-espectrometría de masas (MEFS-CG-EM). TIP Revista Especializada En Ciencias Químico-Biológicas 18:29–42

Qiao F, Gao M, Yan H (2016) Molecularly imprinted ionic liquid magnetic microspheres for the rapid isolation of organochlorine pesticides in environmental water. J Sep Sci 39:1310–1315

Renkecz T, László K, Horváth V (2014) Molecularly imprinted microspheres prepared by precipitation polymerization at high monomer concentrations. Molecular Imprinting 2:1–17

Rivera-Jaimes JA, Postigo C, Melgoza-Alemán RM, Aceña J, Barceló D, de Alda ML (2018) Study of pharmaceuticals in surface and wastewater from Cuernavaca, Morelos, Mexico: occurrence and environmental risk assessment. Sci Total Environ 613:1263–1274

Sellergren B, Shea KJ (1993) Influence of polymer morphology on the ability of imprinted network polymers to resolve enantiomers. J Chromatogr A 635:31–49

Shamsayei M, Yamini Y, Asiabi H, Safari M (2018) On-line packed magnetic in-tube solid phase microextraction of acidic drugs such as naproxen and indomethacin by using Fe3O4@SiO2@layered double hydroxide nanoparticles with high anion exchange capacity. Microchim Acta 185:192

Soto ML, Moure A, Domínguez H, Parajó JC (2011) Recovery, concentration and purification of phenolic compounds by adsorption: a review. J Food Eng 105:1–27

Surikumaran H, Mohamad S, Sarih NM (2014) Molecular imprinted polymer of methacrylic acid functionalised β-cyclodextrin for selective removal of 2, 4-dichlorophenol. Int J Mol Sci 15:6111–6136

Świacka K, Michnowska A, Maculewicz J, Caban M, Smolarz K (2021) Toxic effects of NSAIDs in non-target species: a review from the perspective of the aquatic environment. Environ Pollut 273:115891

Tabaraki R, Sadeghinejad N (2020) Preparation and application of magnetic molecularly imprinted polymers for rutin determination in green tea. Chemical Papers 74(6):1937–1944

Vargas-Berrones K, Bernal-Jácome L, Díaz de León-Martínez L, Flores-Ramírez R (2020) Emerging pollutants (EPs) in Latin América: a critical review of under-studied EPs, case of study -nonylphenol. Sci Total Environ 726:138493

Wang C, Ding C, Wu Q, Xiong X (2019) Molecularly imprinted polymers with dual template and bifunctional monomers for selective and simultaneous solid-phase extraction and gas chromatographic determination of four plant growth regulators in plant-derived tissues and foods. Food Anal Methods 12:1160–1169

Wang H, Xi H, Xu L, Jin M, Zhao W, Liu H (2021) Ecotoxicological effects, environmental fate and risks of pharmaceutical and personal care products in the water environment: a review. Sci Total Environ 147819

Wojcieszyńska D, Guzik U (2020) Naproxen in the environment: its occurrence, toxicity to nontarget organisms and biodegradation. Appl Microbiol Biotechnol 104:1849–1857

Wu K, Wang Y, Hwu W (2003) FTIR and TGA studies of poly (4-vinylpyridine-co-divinylbenzene)–Cu (II) complex. Polym Degrad Stab 79:195–200

Yan J, Lin W, Gao Z, Ren Y (2021) Use of selected NSAIDs in Guangzhou and other cities in the world as identified by wastewater analysis. Chemosphere 130529

Zheng L, Wang H, Cheng X (2018) Molecularly imprinted polymer nanocarriers for recognition and sustained release of diclofenac. Polym Adv Technol 29:1360–1371

Zhou Y, Xu J, Lu N, Wu X, Zhang Y, Hou X (2021) Development and application of metal-organic framework@ GA based on solid-phase extraction coupling with UPLC-MS/MS for the determination of five NSAIDs in water. Talanta 225:121846